

Dissolution of Two-Component Solids

SHIRISH A. SHAH * and EUGENE L. PARROTT *

Abstract □ The dissolution rates of compressed two-component mixtures were investigated. A good correlation between the composition of the solid and its observed dissolution rate was demonstrated by regression analysis. A model for dissolution was applied to compressed mixtures of aspirin-salicylic acid, aspirin-phenacetin, phenacetin-caffeine, and aspirin and caffeine (the last mixture complexes in solution).

Keyphrases □ Dissolution—compressed two-component mixtures, rate correlated with composition □ Solids, two component—dissolution rate correlated with composition □ Aspirin—compressed mixtures with salicylic acid, phenacetin, or caffeine, dissolution rates compared □ Salicylic acid—compressed mixture with aspirin, dissolution rate compared to other mixtures □ Phenacetin—compressed mixtures with aspirin or caffeine, dissolution rates compared □ Caffeine—compressed mixtures with phenacetin or aspirin, dissolution rates compared

The models and kinetics of dissolution for pure materials have received considerable attention in the past 2 decades, but much less attention has been given to models of dissolution from multicomponent systems. An early pharmaceutical study of the dissolution of a two-component system was reported in which the dissolution rates of several poorly soluble weak acids and trisodium phosphate in various mole fractions were studied (1). As the mole fraction of the acid was increased, the dissolution rate increased to a maximum rate; then a further increase in the mole fraction of the acid decreased the dissolution rate.

The dissolution rates of salicylic acid and povidone from compressed disks also were reported (2). Diffusion models were proposed (3) for the dissolution of non-disintegrating polyphasic mixtures, which contained noninteracting components and complexing components. This approach also has been applied to mixtures of polymorphs (4).

Because the relationship of the dissolution rate of a tableted material to compressional force has not been clearly defined, it was desirable to determine this relationship for the materials used in this study of the dissolution kinetics of two-component systems. Increasing precompressional force caused an increase in the dissolution rate of salicylic acid (5). The $t_{50\%}$ decreased for two conventional sulfamethazine tablet formulations and increased for another formulation with increased compressional force. The effect of formulation was also suggested by Khan and Rhodes (7), who reported that an increase in compressional force enhanced the dissolution rate for dicalcium phosphate dihydrate systems but decreased it for microcrystalline cellulose systems. Similarly, Knoechel *et al.* (8) found that, although force influenced the dissolution rate, the formulation and particular medicinal compound had a greater effect on it.

A steady increase in the dissolution rate was found with increasing compressional force until a maximal value, coinciding with the maximum apparent density, was reached (9, 10). An increase in the dissolution rate

with an increased compressional force to a maximum and then a decrease with a further increase in compressional force were reported (11). Other studies (12, 13) reported one or two maxima. In contrast, a decrease in the dissolution rate with increasing compressional force to a minimum and then an increase in the dissolution rate with a further increase in compressional force were observed (14, 15).

Kanke and Sekiguchi (16) confirmed earlier reports (17, 18) that for benzoic acid the force exerted no influence on the dissolution rate and that the size of sulfathiazole particles being compressed had no effect on the dissolution rate.

The purpose of this investigation was to apply a diffusion layer model to the dissolution of compressed two-component solids containing interacting and non-interacting components.

EXPERIMENTAL

Preparation of Compressed Spheres and Measurement of Densities—Material that passed through an 80-mesh sieve but was retained on a 100-mesh sieve was compacted by means of a hydraulic press¹ into compressed spheres having a diameter of 1.270 ± 0.005 cm. Depending on the compressibility of the material, compressional forces ranged from 270 to 10,900 kg. The apparent density of the compressed spheres was determined by the displacement method. The sphere was suspended by a short, thin wire from an analytical balance, and its weight was measured when the sphere was immersed in a saturated solution of the material comprising the sphere. The apparent density, ρ_a , was calculated from:

$$\rho_a = \frac{w_{\text{air}}}{w_{\text{air}} - w_{\text{sol}}} \rho_{\text{sol}} \quad (\text{Eq. 1})$$

where ρ_{sol} is the density of the saturated solution, and w_{air} and w_{sol} are the weights of the sphere in air and the saturated solution, respectively. The true density of the material was determined by means of a pycnometer using *n*-heptane. The percent porosity was calculated by:

$$\text{percent porosity} = 100 (1 - \rho_a/\rho) \quad (\text{Eq. 2})$$

Dissolution Rate—The dissolution rate was determined in distilled water at $25 \pm 0.1^\circ$, as previously described (17, 19), under conditions where the concentration of the solute did not exceed 5% of its solubility. The dissolution apparatus consisted of a 2-liter beaker in which a 3.0×1.5 -cm stainless steel paddle was positioned 6.0 cm from the bottom of the beaker. A speed of 324 rpm and a volume of 2 liters of distilled water were used. Each sphere was weighed initially and upon withdrawal from the dissolution medium at appropriate times.

The dissolution medium was analyzed for the component(s) of the sphere by a UV spectrophotometric method. The amount of each component was determined, and the total solid dissolved was calculated. In all analyses, a material balance was demonstrated between the loss of weight of the solid and the components in solution. For each time interval, the difference between the cube root of the initial weight of the sphere and the cube root of the weight at each interval of time was plotted against time. By knowing the shape-volume factor (4.85 for a sphere) and the density of the material, the dissolution rate was calculated (17).

Analytical Procedures—For single-component spheres of benzoic acid, aspirin, and salicylic acid, standard concentration-absorbance

¹ Carver press, model C.

curves were prepared at 273, 275, and 297 nm, respectively. All standard curves exhibited a Beer's law relationship in the concentration range employed. At each time interval during dissolution, an aliquot was withdrawn by a pipet fitted with a filter. If required, the aliquot was diluted with distilled water, and the absorbance was measured spectrophotometrically at the appropriate wavelength.

For multicomponent spheres, a simultaneous analysis was made by use of simultaneous equations (20, 21). For aspirin and salicylic acid, a series of aqueous solutions of known concentrations of aspirin and salicylic acid was prepared, and the absorbance was measured at 275 and 297 nm. From the data, coefficients of the simultaneous equations were determined. Since absorbance is directly proportional to absorptivity and concentration, if the length of the absorbing solution is constant:

$$C_{ASA} = \frac{a_{2\lambda_2}A_1 - a_{2\lambda_1}A_2}{a_{1\lambda_1}a_{2\lambda_2} - a_{2\lambda_1}a_{1\lambda_2}} \quad (\text{Eq. 3})$$

and:

$$C_{SAL} = \frac{a_{1\lambda_1}A_2 - a_{1\lambda_2}A_1}{a_{1\lambda_1}a_{2\lambda_2} - a_{2\lambda_1}a_{1\lambda_2}} \quad (\text{Eq. 4})$$

where C_{ASA} and C_{SAL} are the concentrations of aspirin and salicylic acid, respectively; A_1 and A_2 are the absorbances at 275 and 297 nm, respectively; $a_{1\lambda_1}$ and $a_{1\lambda_2}$ are the molar absorptivities for aspirin at 275 and 297 nm, respectively; and $a_{2\lambda_1}$ and $a_{2\lambda_2}$ are the molar absorptivities for salicylic acid at 275 and 297 nm, respectively. Substitution of experimental values into Eqs. 3 and 4 yielded:

$$C_{ASA} = (1.3228A_1 - 0.4499A_2) \text{ mM} \quad (\text{Eq. 5})$$

and:

$$C_{SAL} = (0.2961A_2 - 0.0352A_1) \text{ mM} \quad (\text{Eq. 6})$$

For convenience, Eqs. 5 and 6 were expressed in milligrams per milliliter:

$$C_{ASA} = (0.2383A_1 - 0.0811A_2) \text{ mg/ml} \quad (\text{Eq. 7})$$

and:

$$C_{SAL} = (0.0409A_2 - 0.00486A_1) \text{ mg/ml} \quad (\text{Eq. 8})$$

At each time interval during dissolution, an aliquot was withdrawn and, after dilution with distilled water if required, the absorbance was measured² at 275 and 297 nm. The concentrations of aspirin and salicylic acid in solution were determined using Eqs. 7 and 8.

By using the method described previously (22), the amount of salicylic acid in the batch of aspirin used was 0.07%. Since aspirin hydrolyzes, the extent of hydrolysis during the dissolution interval was considered. At 30-, 60-, and 90-min intervals, colorimetric analysis (22) and UV spectroscopy detected no salicylic acid. Since both methods detected no salicylic acid and the usual interval was 15 min, aspirin hydrolysis during the dissolution interval apparently did not occur to a significant extent to affect dissolution values.

The concentrations of caffeine, phenacetin, and aspirin in solution were determined spectrophotometrically by the method of Clayton and Thiers (23). In the manner previously described, coefficients for simultaneous equations were determined. The simultaneous equations used in studying the dissolution of aspirin-caffeine spheres are:

$$C_{ASA} = (0.05046A_1 - 0.00158A_2) \text{ mg/ml} \quad (\text{Eq. 9})$$

and:

$$C_{CAF} = (0.019904A_2 - 0.006078A_1) \text{ mg/ml} \quad (\text{Eq. 10})$$

where A_1 is the absorbance of hydrolyzed solution at 301 nm, and A_2 is the absorbance of the acidic solution at 273 nm.

Simultaneous equations for the analysis of aspirin and phenacetin dissolved from an aspirin-phenacetin sphere are:

$$C_{ASA} = (0.05035A_1 - 0.00166A_2) \text{ mg/ml} \quad (\text{Eq. 11})$$

and:

$$C_{PH} = (0.01632A_2 - 0.00521A_1) \text{ mg/ml} \quad (\text{Eq. 12})$$

where A_1 is the absorbance of the hydrolyzed solution at 301 nm, and A_2 is the absorbance of the acidic solution at 250 nm.

Table I—Relationship of Compressional Force to Dissolution Rate, Apparent Density, and Percent Porosity

Force, kg	Dissolution Rate ^a , g/hr/cm ²	Apparent Density, g/ml	Porosity, %
Benzoic Acid			
900	0.0429	1.29	5.1
2,270	0.0405	1.31	3.7
4,540	0.0408	1.31	3.7
6,800	0.0429	1.31	3.7
9,080	0.0450	1.31	3.7
10,900	0.0429	1.31	3.7
Salicylic Acid			
270	0.0275	1.19	20.1
454	0.0283	1.24	16.8
910	0.0276	1.31	12.1
1,360	0.0274	1.34	10.1
1,800	0.0278	1.36	8.7
2,270	0.0288	1.38	7.4
4,450	0.0273	1.39	6.7
6,800	0.0270	1.40	6.0
9,080	0.0276	1.40	6.0
10,900	0.0281	1.39	6.7
Aspirin			
270	0.0428	1.30	9.1
454	0.0440	1.32	7.7
910	0.0438	1.35	5.6
1,360	0.0435	1.36	4.9
1,800	0.0432	1.36	4.9
2,270	0.0446	1.37	4.2
4,450	0.0430	1.38	3.5
6,800	0.0429	1.38	3.5
9,080	0.0429	1.38	3.5
10,900	0.0432	1.37	4.2

^a Average of two determinations.

Simultaneous equations for the analysis of phenacetin and caffeine dissolved from a phenacetin-caffeine sphere are:

$$C_{PH} = (0.01762A_1 - 0.00587A_2) \text{ mg/ml} \quad (\text{Eq. 13})$$

and:

$$C_{CAF} = (0.02145A_2 - 0.00522A_1) \text{ mg/ml} \quad (\text{Eq. 14})$$

where A_1 and A_2 are the absorbances of the acidic solution at 250 and 273 nm, respectively.

RESULTS AND DISCUSSION

Influence of Compressional Force on Apparent Density, Porosity, and Dissolution Rate—Numerous reports (8, 9, 24, 25) showed the relationship of porosity and apparent density to the force of compression of tablets. The data in Tables I and II for the com-

Table II—Relationship of Compressional Force to Dissolution Rate, Apparent Density, and Percent Porosity of Equimolar Binary Mixtures

Force, kg	Dissolution Rate ^a , g/hr/cm ²	Apparent Density, g/ml	Porosity, %
Aspirin and Salicylic Acid			
270	—	1.24	15.1
454	—	1.32	9.6
910	0.0484	1.35	7.5
4,540	0.0498	1.39	4.8
10,900	0.0480	1.40	4.1
Aspirin and Caffeine			
910	0.2171	1.33	8.3
2,270	—	1.34	7.6
4,540	0.2207	1.38	4.8
9,080	—	1.40	3.4

^a Average of two determinations.

² Beckman DU.

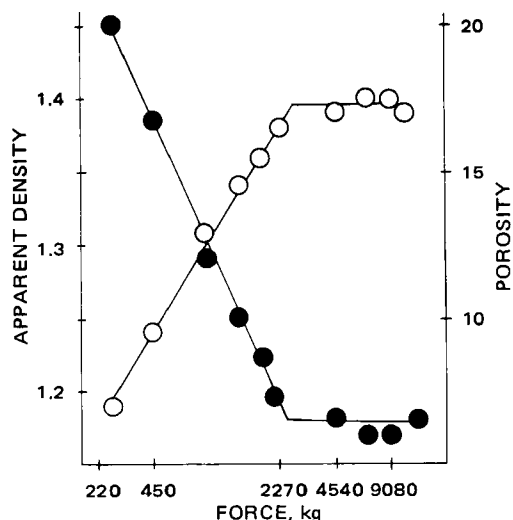


Figure 1—Influence of compressional force on the apparent density and porosity of salicylic acid. Key: O, apparent density; and ●, porosity.

pressed spheres of benzoic acid, salicylic acid, aspirin, an equimolar mixture of aspirin and caffeine, and an equimolar mixture of aspirin and salicylic acid are in agreement with these reports that the apparent density is increased to an asymptotic value as the compressional force is increased. The apparent density is linearly related to the logarithm of the compressional force to a maximal value, as illustrated for salicylic acid in Fig. 1. The porosity of the sphere is decreased as the compressional force is increased. The porosity is linearly related to the logarithm of the compressional force to a minimum porosity (Fig. 1).

Examination of Tables I and II shows that, under essentially sink conditions, the dissolution rate is independent of compressional force for nondisintegrating spheres of benzoic acid, salicylic acid, aspirin, an equimolar mixture of aspirin and salicylic acid, and an equimolar mixture of aspirin and caffeine. Thus, it appears that, in this dissolution study of nondisintegrating solids, the compressional force and the apparent density are insignificant factors and need not be rigidly controlled.

Regression Analysis of Dissolution—Aspirin and salicylic acid

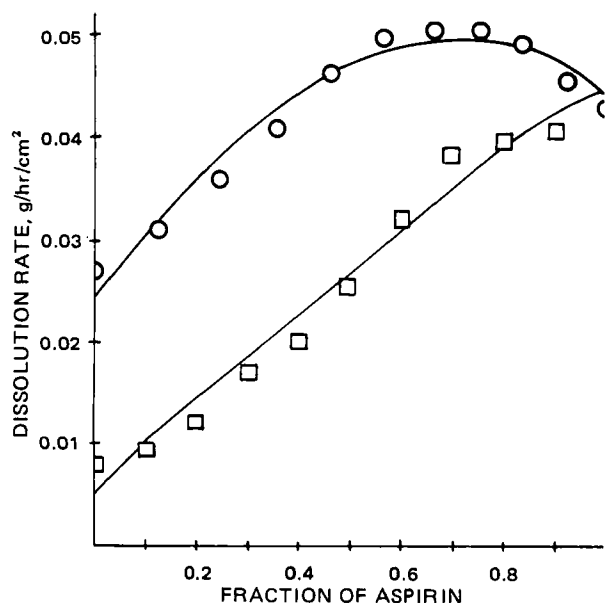


Figure 2—Comparison of experimental dissolution rates of compressed mixtures and regression equation represented by the smooth curves. Key: O, aspirin and salicylic acid; and □, aspirin and phenacetin.

Table III—Composition and Observed Dissolution Rate of Aspirin and Salicylic Acid Mixtures Compressed at 4540 kg

Mole Fraction		Mass Fraction		Dissolution Rate, g/hr/cm ²		
N_{ASA}	N_{SAL}	F_{ASA}	F_{SAL}	ASA	SAL	Sphere
1.0	0	1.000	0	0.0430	—	0.0430
0.9	0.1	0.922	0.078	0.0423	0.0036	0.0459
0.8	0.2	0.839	0.161	0.0415	0.0080	0.0495
0.7	0.3	0.753	0.247	0.0382	0.0125	0.0507
0.6	0.4	0.662	0.338	0.0336	0.0171	0.0507
0.5	0.5	0.566	0.434	0.0282	0.0216	0.0498
0.4	0.6	0.465	0.535	0.0215	0.0248	0.0463
0.3	0.7	0.359	0.641	0.0148	0.0264	0.0412
0.2	0.8	0.246	0.754	0.0088	0.0271	0.0359
0.1	0.9	0.127	0.873	0.0039	0.0272	0.0311
0	1.0	0	1.000	—	0.0272	0.0272

mixtures of various mole fractions were compressed at 4540 kg into spheres. During dissolution of the compressed sphere, disintegration did not occur; each retained its spherical shape as dissolution occurred. The compositions and dissolution rates of aspirin-salicylic acid spheres are given in Table III. Since the experimentally determined ratio of the components in solution was the same as the ratio of the components in the solid, the dissolution rate may be calculated by multiplying the dissolution rate of the sphere by the mass fraction of the component in the solid.

A stepwise regression analysis was performed using the STEP-REGN program. The regression equation for the dissolution rate, R , of aspirin-salicylic acid spheres is:

$$R = (0.02438 + 0.07048F_{ASA}) - 0.05008F_{ASA}^2 \text{ g/hr/cm}^2 \quad (\text{Eq. 15})$$

where F_{ASA} is the mass fraction of aspirin in the aspirin-salicylic acid mixture. The coefficient of determination, r^2 , is 0.9466, a value that indicates a good correlation of the experimental data with the regression equation. The experimental dissolution rate and the dissolution rate calculated by the regression equation are shown in Fig. 2.

In a similar manner, the dissolution rates of aspirin-phenacetin spheres of various mole fractions compressed at 4540 kg were determined (Table IV). The regression equation for the dissolution rate of aspirin-phenacetin spheres is:

$$R = (0.00541 + 0.04483F_{ASA}) - 0.00492F_{ASA}^2 \text{ g/hr/cm}^2 \quad (\text{Eq. 16})$$

The r^2 value is 0.9733, a value that indicates an excellent correlation

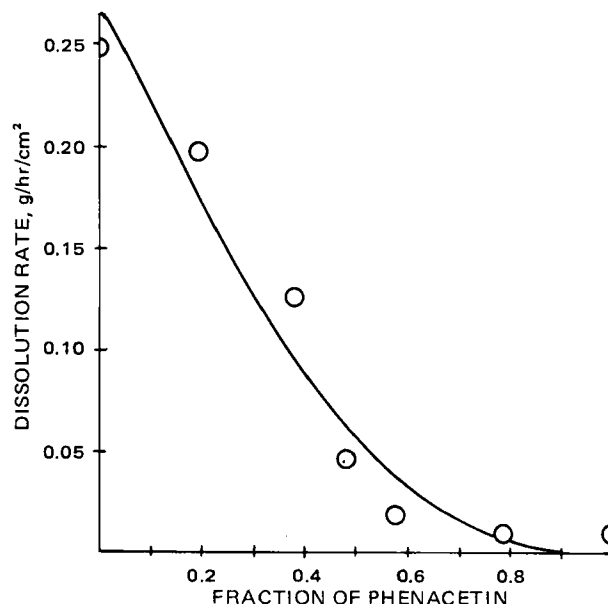


Figure 3—Comparison of experimental dissolution rates of compressed phenacetin and caffeine mixtures and regression equation represented by the smooth curve.

Table IV—Composition and Observed Dissolution Rate of Aspirin and Phenacetin Mixtures Compressed at 4540 kg

Mole Fraction		Mass Fraction		Dissolution Rate, g/hr/cm ²		
N _{ASA}	N _{PH}	F _{ASA}	F _{PH}	ASA	PH	Sphere
1.0	0	1.000	0	0.0430	—	0.0430
0.9	0.1	0.900	0.100	0.0370	0.0041	0.0411
0.8	0.2	0.801	0.199	0.0320	0.0079	0.0399
0.7	0.3	0.701	0.299	0.0269	0.0115	0.0384
0.6	0.4	0.601	0.399	0.0195	0.0129	0.0324
0.5	0.5	0.501	0.499	0.0130	0.0125	0.0255
0.4	0.6	0.401	0.599	0.0081	0.0120	0.0201
0.3	0.7	0.301	0.699	0.0051	0.0120	0.0171
0.2 ^a	0.8	0.201	0.799	0.0025	0.0098	0.0123
0.1 ^b	0.9	0.100	0.900	0.0010	0.0086	0.0096
0	1.0 ^b	0	1.000	—	0.0080	0.0080

^a Compressed at 680 kg. ^b Melt method.

of the experimental data with the regression equation. The experimental dissolution rate and the dissolution rate calculated by the regression equation are shown in Fig. 2.

Attempts to compress phenacetin and caffeine mixtures were unsuccessful, and a melt process was used. Mixtures of phenacetin and caffeine were compressed at 4540 kg for 5 min within a hot stage at 265°. The compositions and dissolution rates are given in Table V. The regression equation for the dissolution rate of phenacetin-caffeine spheres is:

$$R = (0.26689 - 0.54995F_{PH}) + 0.28451F_{PH}^2 \text{ g/hr/cm}^2 \quad (\text{Eq. 17})$$

where F_{PH} is the mass fraction of the phenacetin in the phenacetin-caffeine mixture. The r^2 value is 0.9562, a value that indicates good correlation of the experimental data with the regression equation. The experimental dissolution rate and the dissolution rate calculated by the regression equation are shown in Fig. 3.

Aspirin and caffeine mixtures of various mole fractions were compressed at 4540 kg into spheres. The compositions and dissolution rates are given in Table VI. The regression equation for the dissolution rate of aspirin-caffeine spheres is:

$$R = (0.27378 + 0.0924F_{ASA}) - 0.3809F_{ASA}^2 \text{ g/hr/cm}^2 \quad (\text{Eq. 18})$$

The r^2 value for the aspirin-caffeine system is 0.8199. The experimental dissolution rates and the dissolution rates calculated by the regression equation are shown in Fig. 4.

Dissolution of Noninteracting Solids—Higuchi *et al.* (3) presented a theory for the dissolution of polyphasic mixtures using a diffusion layer model. For a mixture in which F_A and F_B are the amounts of components A and B, both components tend to dissolve at rates proportional to their respective solubilities, C_A and C_B , and diffusion coefficients, D_A and D_B . At some composition (critical mixture), the two components always coexist at the solid-liquid interface, and the dissolution rates are proportional to their relative amounts in the mixture. Thus:

$$\frac{F_A}{F_B} = \frac{D_A C_A}{D_B C_B} \quad (\text{Eq. 19})$$

At other compositions after some time, one component is dissolved from the solid-liquid interface fast enough to leave a layer of the other component. If:

$$\frac{F_A}{F_B} > \frac{D_A C_A}{D_B C_B} \quad (\text{Eq. 20})$$

component B dissolves fast enough to leave a layer of A at the solid-liquid interface. The dissolution rates are:

$$R_A = \frac{D_A C_A}{h} \quad (\text{Eq. 21})$$

where h is the thickness of the effective diffusion layer, and:

$$R_B = \frac{F_B}{F_A} R_A \quad (\text{Eq. 22})$$

If:

$$\frac{F_A}{F_B} < \frac{D_A C_A}{D_B C_B} \quad (\text{Eq. 23})$$

component A dissolves fast enough to leave a layer of B at the solid-liquid interface. The dissolution rates are:

Table V—Composition and Observed Dissolution Rate of Phenacetin and Caffeine Mixtures Prepared by the Melt Method

Mole Fraction		Mass Fraction		Dissolution Rate, g/hr/cm ²		
N _{PH}	N _{CAF}	F _{PH}	F _{CAF}	PH	CAF	Sphere
1.0	0	1.000	0	0.0080	—	0.0080
0.8	0.2	0.787	0.213	0.0091	0.0024	0.0115
0.6	0.4	0.581	0.419	0.0126	0.0090	0.0216
0.5	0.5	0.480	0.520	0.0227	0.0245	0.0472
0.4	0.6	0.381	0.619	0.0482	0.0782	0.1264
0.2	0.8	0.188	0.812	0.0372	0.1612	0.1984
0	1.0	0	1.000	—	0.2493	0.2493

Table VI—Composition and Observed Dissolution Rate of Aspirin and Caffeine Mixtures Compressed at 4540 kg

Mole Fraction		Mass Fraction		Dissolution Rate, g/hr/cm ²		
N _{ASA}	N _{CAF}	F _{ASA}	F _{CAF}	ASA	CAF	Sphere
1.0	0	1.000	0	0.0430	—	0.0430
0.9	0.1	0.893	0.107	0.0450	0.0050	0.0500
0.8	0.2	0.788	0.212	0.0510	0.0140	0.0650
0.7	0.3	0.684	0.316	0.0680	0.0310	0.0990
0.6	0.4	0.582	0.418	0.0940	0.0680	0.1620
0.5	0.5	0.481	0.519	0.1045	0.1125	0.2170
0.4	0.6	0.382	0.618	0.1250	0.2010	0.3260
0.3	0.7	0.284	0.716	0.0900	0.2250	0.3150
0.2	0.8	0.188	0.812	0.0590	0.2560	0.3150
0.1 ^a	0.9	0.094	0.906	0.0260	0.2530	0.2790
0	1.0	0	1.000	—	0.2152	0.2152

^a Compressed at 3600 kg.

$$R_B = \frac{D_B C_B}{h} \quad (\text{Eq. 24})$$

and:

$$R_A = \frac{F_A}{F_B} R_B \quad (\text{Eq. 25})$$

Application of the theory can be demonstrated for the compressed aspirin-salicylic acid spheres. Edwards (26) reported that the solubility of aspirin, C_{ASA} , in water at 25° was 4.44×10^{-3} g/ml and that the diffusion coefficient of aspirin, D_{ASA} , in water at 25° was 8.01×10^{-6} cm²/sec. Hall (27) reported that the solubility of salicylic acid,

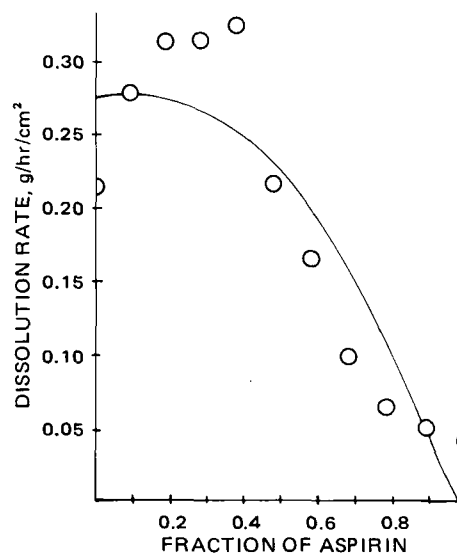


Figure 4—Comparison of experimental dissolution rates of compressed aspirin and caffeine mixtures and regression equation represented by the smooth curve.

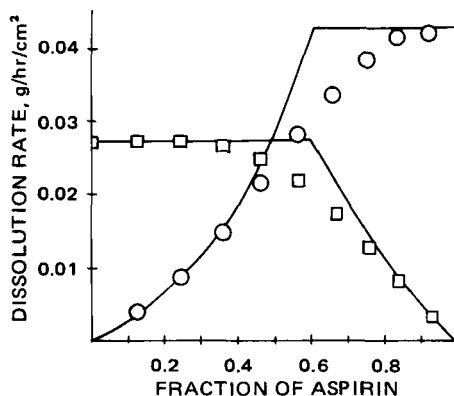


Figure 5—Comparison of observed dissolution rates of the components of compressed aspirin and salicylic acid mixtures and smooth curve representing the theoretical rates. Key: O, aspirin; and □, salicylic acid.

C_{SAL} in water at 25° was 2.24×10^{-3} g/ml. Mullin and Cook (28) reported that the diffusion coefficient of salicylic acid, D_{SAL} , in water at 25° was 10.12×10^{-6} cm²/sec. The thickness of the effective diffusion layer was chosen as 30 μm (29).

For the aspirin and salicylic acid mixture, the critical ratio is:

$$\frac{F_{ASA}}{F_{SAL}} = \frac{D_{ASA}C_{ASA}}{D_{SAL}C_{SAL}} \quad (\text{Eq. 26a})$$

$$\frac{F_{ASA}}{F_{SAL}} = \frac{(8.01 \times 10^{-6})(4.44 \times 10^{-3})}{(10.12 \times 10^{-6})(2.24 \times 10^{-3})} \quad (\text{Eq. 26b})$$

$$\frac{F_{ASA}}{F_{SAL}} = \frac{0.611}{0.389} \quad (\text{Eq. 26c})$$

At the critical ratio, the dissolution rates are:

$$R_{ASA} = \frac{D_{ASA}C_{ASA}}{h} \quad (\text{Eq. 27a})$$

$$R_{ASA} = \frac{(8.01 \times 10^{-6})(4.44 \times 10^{-3})}{3 \times 10^{-3}} \quad (\text{Eq. 27b})$$

$$R_{ASA} = 1.18548 \times 10^{-5} \text{ g/sec/cm}^2 \text{ (0.0427 g/hr/cm}^2\text{)} \quad (\text{Eq. 27c})$$

and:

$$R_{SAL} = \frac{D_{SAL}C_{SAL}}{h} \quad (\text{Eq. 28a})$$

$$R_{SAL} = \frac{(10.12 \times 10^{-6})(2.24 \times 10^{-3})}{3 \times 10^{-3}} \quad (\text{Eq. 28b})$$

$$R_{SAL} = 7.556 \times 10^{-6} \text{ g/sec/cm}^2 \text{ (0.0272 g/hr/cm}^2\text{)} \quad (\text{Eq. 28c})$$

For compositions of $F_{ASA} > 0.611$, the condition described by Eq. 20 exists so that aspirin is present to a greater extent on the solid-liquid interface. For example, at $F_{ASA} = 0.753$ and $F_{SAL} = 0.247$, the dissolution rate as expressed by Eq. 21 for aspirin is:

$$R_{ASA} = \frac{D_{ASA}C_{ASA}}{h} \quad (\text{Eq. 29a})$$

$$R_{ASA} = \frac{(8.01 \times 10^{-6})(4.44 \times 10^{-3})}{3 \times 10^{-3}} \quad (\text{Eq. 29b})$$

$$R_{ASA} = 11.8548 \times 10^{-6} \text{ g/sec/cm}^2 \text{ (0.0427 g/hr/cm}^2\text{)} \quad (\text{Eq. 29c})$$

and the dissolution rate as expressed by Eq. 22 for salicylic acid is:

$$R_{SAL} = \frac{F_{SAL}}{F_{ASA}} R_{ASA} \quad (\text{Eq. 30a})$$

$$R_{SAL} = \frac{0.247}{0.753} (0.0427) \quad (\text{Eq. 30b})$$

$$R_{SAL} = 0.0082 \text{ g/hr/cm}^2 \quad (\text{Eq. 30c})$$

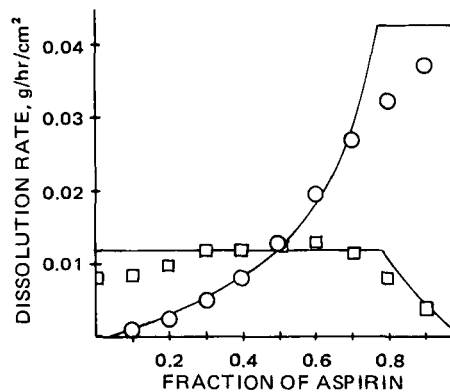


Figure 6—Comparison of observed dissolution rates of the components of compressed aspirin and phenacetin mixtures and smooth curve representing the theoretical rates. Key: O, aspirin; and □, phenacetin.

For compositions of $F_{ASA} < 0.611$, the condition described by Eq. 23 exists so that salicylic acid exists to a greater extent on the solid-liquid interface. For example, at $F_{ASA} = 0.465$ and $F_{SAL} = 0.535$, the dissolution rate as expressed by Eq. 24 for salicylic acid is:

$$R_{SAL} = \frac{D_{SAL}C_{SAL}}{h} \quad (\text{Eq. 31a})$$

$$R_{SAL} = \frac{(10.12 \times 10^{-6})(2.24 \times 10^{-3})}{3 \times 10^{-3}} \quad (\text{Eq. 31b})$$

$$R_{SAL} = 7.5563 \times 10^{-6} \text{ g/sec/cm}^2 \text{ (0.0272 g/hr/cm}^2\text{)} \quad (\text{Eq. 31c})$$

and the dissolution rate as expressed by Eq. 25 for aspirin is:

$$R_{ASA} = \frac{F_{ASA}}{F_{SAL}} R_{SAL} \quad (\text{Eq. 32a})$$

$$R_{ASA} = \frac{0.465}{0.641} (0.0272) \quad (\text{Eq. 32b})$$

$$R_{ASA} = 0.0236 \text{ g/hr/cm}^2 \quad (\text{Eq. 32c})$$

The dissolution rates calculated for various compositions are compared to the experimental dissolution rates of Table III in Fig. 5.

In a similar manner, the theoretical dissolution rates were calculated for aspirin and phenacetin mixtures. Seidell (30) reported that the solubility of phenacetin, C_{PH} , in water at 25° was 1.1×10^{-3} g/ml. Shively and Kildsig (31) reported that the diffusion coefficient of phenacetin, D_{PH} , in water at 30° was 9×10^{-6} cm²/sec. The dissolution rates calculated for various compositions of aspirin and phenacetin are compared to the experimental dissolution rates of Table IV in Fig. 6.

In Figs. 5 and 6, the observed dissolution rates approximate the smooth curves representing the theoretical dissolution rates, thereby substantiating the model. At the critical ratio, deviation probably is caused by small local variations in compositions. It was reported (3) that solid mixtures prepared by a melt method deviate less because they are more homogeneous.

The theoretical dissolution rates were calculated for phenacetin and caffeine mixtures. Paruta *et al.* (32) reported that the solubility of caffeine, C_{CAF} , in water at 25° was 23.2×10^{-3} g/ml. McCabe (33) reported that the diffusion coefficient of caffeine, D_{CAF} , in water at 25° was 6.79×10^{-6} cm²/sec. The dissolution rates calculated for various compositions of caffeine and phenacetin are compared to the experimental dissolution rates of Table V in Fig. 7.

As shown in Fig. 7, the theoretical and observed dissolution rates of caffeine and phenacetin are similar for mixtures containing more than half phenacetin. For compositions containing a large fraction of caffeine, there is deviation. Caffeine is 21 times more soluble than phenacetin, and it readily dissolves to produce a rough surface with minute flaking. As a result, the effective surface area is increased, and the observed dissolution of both components is faster than predicted by the model.

The dissolution rate of caffeine from solids prepared using a melt

method was reported as 20% faster than from a compressed disk, and the assumption was that the solubility of the melt was greater (3). Experimentally, the dissolution rate of spheres made by the melt method was 16% faster than by compression only. This result could also contribute to the faster observed dissolution rate of the phenacetin spheres, which contain a large fraction of caffeine.

Dissolution of Interacting Solids—Aspirin and caffeine in solution undergo the interaction: aspirin + caffeine → (aspirin-caffeine). The equilibrium constant:

$$K = \frac{(\text{aspirin-caffeine})}{(\text{aspirin})(\text{caffeine})} \quad (\text{Eq. 33})$$

was reported as 17.4 liters/mole (34).

The model of Higuchi was extended to two-component systems in which the components interacted to form a complex and was supported by experimental data obtained from benzocaine and caffeine mixtures (3). When assuming that the interaction is represented by $B + C = BC$, the equilibrium constant is:

$$K = \frac{C_{BC}}{C_B C_C} \quad (\text{Eq. 34})$$

where C_B , C_C , and C_{BC} are the concentrations of components B, C, and BC, respectively.

The composition of the critical ratio is:

$$\frac{N_B}{N_C} = \frac{D_B C_B + D_{BC} K C_B C_C}{D_C D_C + D_{BC} K C_B C_C} \quad (\text{Eq. 35})$$

at which the dissolution rates are:

$$R_C = \frac{D_C C_C + D_{BC} K C_B C_C}{h} \quad (\text{Eq. 36})$$

and:

$$R_B = \frac{D_B C_B + D_{BC} K C_B C_C}{h} \quad (\text{Eq. 37})$$

When the ratio of the components is such that pure C is the surface phase, the dissolution rates may be determined by:

$$R_B h = \frac{D_B C_B}{1 - \frac{N_C D_{BC} K C_B}{N_B (D_B + D_{BC} K C_B)}} \quad (\text{Eq. 38})$$

and:

$$R_C h = \frac{D_B C_B}{\frac{N_B}{N_C} - \frac{D_{BC} K C_B}{D_C + D_{BC} K C_B}} \quad (\text{Eq. 39})$$

When the ratio of the components is such that pure B is the surface phase, the dissolution rates may be determined by:

$$R_B h = \frac{D_C C_C}{\frac{N_C}{N_B} - \frac{D_{BC} K C_C}{D_B + D_{BC} K C_C}} \quad (\text{Eq. 40})$$

and:

$$R_C h = \frac{D_C C_C}{1 - \frac{N_B D_{BC} K C_C}{N_C (D_B + D_{BC} K C_C)}} \quad (\text{Eq. 41})$$

For the aspirin and caffeine mixture investigated, the critical ratio calculated by Eq. 35 is $N_{ASA}/N_{CAF} = 0.32/0.68$. The diffusion coefficient of the aspirin-caffeine complex ($D_{ASA-CAF}$) was assumed to be the same as the diffusion coefficient of caffeine because there is a tendency for caffeine to associate as a dimer (35).

At the critical ratio, the dissolution rate of aspirin calculated by Eq. 36 is:

$$R_{ASA}(0.003) = (2.8836 \times 10^{-2})(2.46 \times 10^{-5}) + (2.4444 \times 10^{-2})(17,400)(2.46 \times 10^{-5})(11.95 \times 10^{-5}) \quad (\text{Eq. 42a})$$

$$R_{ASA} = 6.53232 \times 10^{-4} \text{ mole/hr/cm}^2 \text{ (0.1177 g/hr/cm}^2) \quad (\text{Eq. 42b})$$

and the dissolution rate of caffeine calculated by Eq. 37 is:

$$R_{CAF}(0.003) = (2.4444 \times 10^{-2})(11.95 \times 10^{-5}) + (2.4444 \times 10^{-2})(17,400)(2.46 \times 10^{-5})(11.95 \times 10^{-5}) \quad (\text{Eq. 43a})$$

$$R_{CAF} = 1.39 \times 10^{-3} \text{ mole/hr/cm}^2 \text{ (0.2700 g/hr/cm}^2) \quad (\text{Eq. 43b})$$

For compositions of $N_{ASA} > 0.32$, aspirin is the surface phase, and the dissolution rate of aspirin is calculated by Eq. 38. For example,

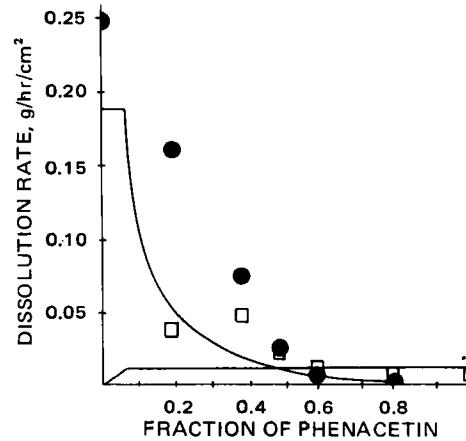


Figure 7—Comparison of observed dissolution rates of the components of compressed caffeine and phenacetin mixtures and smooth curve representing the theoretical rates. Key: ●, caffeine; and ○, phenacetin.

at $N_{ASA} = 0.6$, the dissolution rate of aspirin is:

$$R_{ASA}(0.003) = \frac{(2.46 \times 10^{-5})(2.8836 \times 10^{-2})}{1 - \frac{0.4(2.4444 \times 10^{-2})(17,400)(2.46 \times 10^{-5})}{0.6(2.8836 \times 10^{-2}) + (2.4444 \times 10^{-2})(17,400)(2.46 \times 10^{-5})}} \quad (\text{Eq. 44a})$$

$$R_{ASA} = 2.874667 \times 10^{-4} \text{ mole/hr/cm}^2 \text{ (0.0518 g/hr/cm}^2) \quad (\text{Eq. 44b})$$

In a similar manner, the dissolution rate of caffeine calculated by Eq. 39 is 0.0383 g/hr/cm².

For compositions of $N_{ASA} < 0.32$, caffeine is the surface phase, and the dissolution rate is calculated by Eq. 41. For example, at $N_{ASA} = 0.2$, the dissolution rate of aspirin is 0.0522 g/hr/cm². From Eq. 40, the dissolution rate of caffeine is 0.2250 g/hr/cm².

The dissolution rates calculated for various compositions are compared to the experimental dissolution rates of Table VI in Fig. 8.

As the fraction of aspirin in the mixture is increased, the dissolution rate of aspirin and caffeine is increased to a maximum dissolution rate

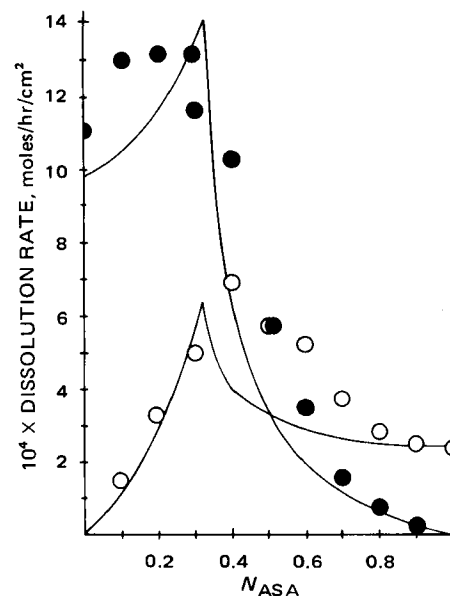


Figure 8—Comparison of observed dissolution rates of the components of compressed aspirin and caffeine mixtures and smooth curve representing the theoretical rates. Key: ○, aspirin; and ●, caffeine.

at the critical ratio, and then a further increase in the fraction of aspirin causes a decrease in the dissolution rates of aspirin and caffeine. The model predicts the observed dissolution rates of aspirin for compositions less than 0.3 and more than 0.8 mass fraction of aspirin. At other compositions, the dissolution rate of aspirin is faster than the theoretical rates. Caffeine has five times as great a solubility as aspirin; since it dissolves faster than the aspirin, minute flaking would occur because the aspirin matrix remaining would be porous and mechanically weak. It is likely that minute particles of aspirin flake from the solid-liquid surface with an increase in the effective surface area of the aspirin and, consequently, a faster observed dissolution rate of aspirin than predicted.

The dissolution rate of caffeine conforms to the model at compositions greater than 0.7 mass fraction of aspirin, but at other compositions the dissolution rate of caffeine is faster than predicted by the model. The increased dissolution rate of caffeine at other compositions may be due to several assumptions. In developing the model, it was assumed that only a 1:1 aspirin-caffeine complex was formed and increased the solubility of the caffeine; however, other complexes may exist (34) and at small fractions of caffeine increase the dissolution rate. The faster dissolution may also occur if the caffeine associates as a dimer or tetramer (35). From 0.4 to 0.6 mass fraction of aspirin, the rough surface caused by minute flaking may also increase the observed dissolution rate of caffeine.

REFERENCES

- (1) E. Nelson, *J. Am. Pharm. Assoc., Sci. Ed.*, **46**, 607(1957).
- (2) M. Gibaldi and H. Weintraub, *J. Pharm. Sci.*, **57**, 832(1968).
- (3) W. I. Higuchi, N. A. Mir, and S. J. Desai, *ibid.*, **54**, 1405(1965).
- (4) W. I. Higuchi, P. D. Bernardo, and S. C. Mehta, *ibid.*, **56**, 200(1967).
- (5) G. L. Levy, J. M. Antkowiak, J. A. Procknal, and D. C. White, *ibid.*, **52**, 1047(1963).
- (6) M. C. B. van Oudtshoorn, F. J. Potgieter, G. J. de Blaey, and J. Polderman, *J. Pharm. Pharmacol.*, **23**, 583(1971).
- (7) K. A. Khan and C. T. Rhodes, *Pharm. Acta Helv.*, **47**, 116(1967).
- (8) E. L. Knoechel, C. C. Sperry, and C. J. Lintner, *J. Pharm. Sci.*, **56**, 116(1967).
- (9) J. Polderman and D. R. Braakman, *J. Pharm. Pharmacol.*, **20**, 323(1968).
- (10) C. J. de Blaey, M. C. B. van Oudtshoorn, and J. Polderman, *Pharm. Weekbl.*, **106**, 589(1971).
- (11) E. Cid and F. Jaminet, *Pharm. Acta Helv.*, **46**, 167(1971).
- (12) H. L. Smith, C. A. Baker, and J. H. Wood, *J. Pharm. Pharmacol.*, **23**, 536(1971).
- (13) D. Ganderton, J. W. Hadgraft, W. T. Respin, and A. G. Thompson, *Pharm. Acta Helv.*, **42**, 152(1963).
- (14) E. R. Kristofferson, *Farm. Aikak.*, **78**, 185(1969).
- (15) C. J. de Blaey, A. B. Weekers-Andersen, and J. Polderman, *Pharm. Weekbl.*, **106**, 893(1971).
- (16) M. Kanke and K. Sekiguchi, *Chem. Pharm. Bull.*, **21**, 871(1973).
- (17) E. L. Parrott, D. E. Wurster, and T. Higuchi, *J. Am. Pharm. Assoc., Sci. Ed.*, **44**, 269(1955).
- (18) G. Milosovich, *J. Pharm. Sci.*, **53**, 484(1964).
- (19) R. J. Braun and E. L. Parrott, *ibid.*, **61**, 175(1972).
- (20) H. H. Willard, L. L. Merritt, and J. A. Dean, "Instrumental Methods of Analysis," Van Nostrand, Princeton, N.J., 1958, p. 120.
- (21) R. B. Tinker and A. J. McBey, *J. Am. Pharm. Assoc., Sci. Ed.*, **43**, 315(1954).
- (22) R. E. Pankratz and F. J. Bandelin, *ibid.*, **41**, 267(1952).
- (23) A. W. Clayton and R. E. Thiers, *J. Pharm. Sci.*, **55**, 404(1966).
- (24) T. Higuchi, A. N. Rao, L. W. Busse, and J. V. Swintosky, *J. Am. Pharm. Assoc., Sci. Ed.*, **42**, 194(1953).
- (25) C. J. Lewis and D. Train, *J. Pharm. Pharmacol.*, **17**, 1(1965).
- (26) L. J. Edwards, *Trans. Faraday Soc.*, **47**, 1191(1951).
- (27) N. A. Hall, *Amer. J. Pharm.*, **132**, 406(1960).
- (28) J. W. Mullin and T. P. Cook, *J. Appl. Chem.*, **15**, 145(1965).
- (29) R. J. Braun and E. L. Parrott, *J. Pharm. Sci.*, **61**, 592(1972).
- (30) A. Seidell, *J. Am. Chem. Soc.*, **92**, 1088(1970).
- (31) C. D. Shively and D. O. Kildsig, *J. Pharm. Sci.*, **61**, 1589(1972).
- (32) A. N. Paruta, B. J. Sciarone, and N. G. Lordi, *ibid.*, **54**, 838(1965).
- (33) M. McCabe, *Biochem. J.*, **127**, 249(1972).
- (34) T. Higuchi and D. A. Zuck, *J. Am. Pharm. Assoc., Sci. Ed.*, **42**, 138(1953).
- (35) D. Guttman and T. Higuchi, *ibid.*, **46**, 4(1957).

ACKNOWLEDGMENTS AND ADDRESSES

Received October 14, 1975, from the College of Pharmacy, University of Iowa, Iowa City, IA 52242

Accepted for publication February 13, 1976.

Abstracted in part from a dissertation submitted by S. A. Shah to the Graduate College, University of Iowa, in partial fulfillment of the Doctor of Philosophy degree requirements.

* Present address: Johnson & Johnson, Raritan, NJ 08869

* To whom inquiries should be directed.